SURFACE, ELECTRON AND ION EMISSION

Phenomenological Theory for the Melting of a Thin Lubricant Film between Two Atomically Smooth Solid Surfaces

I. A. Lyashenko[a], A. V. Khomenko[a]*, and L. S. Metlov[b]**

[a] Sumy State University, Sumy, 40007 Ukraine
[b] Galkin Physicotechnical Institute, National Academy of Sciences of Ukraine,
ul. Rozy Lyuksemburg 72, Donetsk, 83114 Ukraine
e-mail: nabla04@ukr.net

Abstract—A thermodynamic model is developed for the melting of an ultrathin lubricant film squeezed between two atomically smooth solid surfaces. To describe the state of lubricant, an excess volume parameter is introduced; it appears due to the chaos in the structure of a solid body induced by melting. This parameter increases with the total internal energy upon melting. Thermodynamic melting and shear melting are described. The dependences of the friction force on the lubricant temperature and the shear rate of friction surfaces are analyzed. The calculated results are compared to the experimental data.

INTRODUCTION

The boundary friction mode that appears at a lubricant thickness smaller than ten atomic layers is being extensively studied [1]. Experiments demonstrate that a thin lubricant layer exhibits anomalous properties as compared to bulk lubricants [2]. In particular, stick–slip motion inherent in dry friction is detected [2, 3]. This mode is explained as solidification caused by the compression of friction surfaces and subsequent jumplike melting when shear stresses exceed the yield strength ("shear melting").

There exist several phenomenological models that can partly explain the experimental results, namely, thermodynamic [4], mechanical [5–7], and synergetic [8] models. In addition, molecular dynamics simulations were performed [9]. It turns out that a lubricant can provide several kinetic modes that undergo transitions during friction, and these transitions lead to stick-slip friction [2]. The authors of [6] found the following three friction modes: sliding friction at low shear rates, a regular stick-slip mode, and a sliding mode at high shear rates. These modes were supported in numerous experiments [1–3, 10].

In terms of the Lorenz model, the authors of [8] developed the following approach to approximate a viscoelastic medium: the transition of an ultrathin lubricant film from a solidlike into a liquidlike state results from thermodynamic melting and shear melting. These processes, which are caused by the self-organization of shear-stress fields and deformation fields, and the lubricant temperature were described with allowance for the additive noises of these quantities [11, 12] and correlated temperature fluctuations [13]. The causes of the jumplike melting and hysteresis

detected experimentally in [14–16] were considered in [17, 18]. In [17, 18], we also determined the conditions for these features to take place by making allowance for the deformation-induced defect of a shear modulus.

The disadvantages of this model consist in the fact that it does not take into account the load applied to a friction surface and uses a number of approximations to derive basic equations [8]. In this work, we propose a theory based on the expansion of the free energy of the system in powers of parameter f, which represents the excess volume that appears upon the formation of a defect structure in a lubricant during melting. It should be noted that the lubricant has a nonzero shear modulus even in a liquidlike state: it contains elastic stresses. The liquidlike state is interpreted as a plastic flow segment in a stress–strain curve and is characterized by the presence of defects in the lubricant [4].

This approach was applied earlier to describe severe plastic deformation (SPD) processes [19–23]. SPD processes and the processes proceeding in an ultrathin lubricant have many common features, which allow us to assume that this technique can be used in both cases.

BASIC EQUATIONS

In the course of melting of a lubricant thinner than ten molecular layers, its stationary states represent kinetic friction modes rather than being true thermodynamic phases. Therefore, several such states can occur [2]. In this case, researchers use terms solidlike and liquidlike phases rather than solid and liquid phases. The melting of such lubricants is accompanied by an increase in their volume [9] and diffusion coeffi-

cient [9, 24, 25]. Since the volume is an experimentally detected quantity among these two quantities, we introduce parameter f, which has the physical meaning of the excess volume that appears due to the melting-induced chaos in the structure of solids, in order to describe the state of the lubricant. As parameter f increases, the defect density in the lubricant increases, and the lubricant exhibits a kinetic plastic flow mode (liquidlike phase) due to defect transport under the action of applied stresses. In contrast to the order parameter used to describe solid–liquid transition processes, this parameter increases with the total internal energy during such a transition.

We write the expansion of the free energy density by making allowance for the contributions of the elastic components of shear strains ε_{ij}^e and entropy s in the form

$$\Phi = \Phi_0^* + \frac{1}{2}\lambda(\varepsilon_{ii}^e)^2 + \mu(\varepsilon_{ij}^e)^2 - \alpha s^2 + \frac{c}{2}(\nabla f)^2 \qquad (1)$$
$$- \varphi_0 f + \frac{1}{2}\varphi_1 f^2 - \frac{1}{3}\varphi_2 f^3 + \frac{1}{4}\varphi_3 f^4,$$

where Φ_0^*, λ, μ, α, c, φ_0, φ_1, φ_2, and φ_3 are expansion constants. In turn, we have

$$\varphi_0 = \varphi_0^* + \frac{1}{2}\bar{\lambda}(\varepsilon_{ii}^e)^2 + \bar{\mu}(\varepsilon_{ij}^e)^2 + \alpha_\varphi s. \qquad (2)$$

Elastic stresses are taken into account accurate to quadratic contributions through the first two invariants of strain tensor ε_{ii}^e, $(\varepsilon_{ij}^e)^2 = \varepsilon_{ij}^e\varepsilon_{ji}^e$, where summation is meant in repeating indices. The first invariant represents the trace of strain tensor $\varepsilon_{ii}^e = \varepsilon_1^e + \varepsilon_2^e + \varepsilon_3^e$, and the second invariant is expressed as [26]

$$(\varepsilon_{ij}^e)^2 \equiv (\varepsilon_{ll}^e)^2 - 2I_2 = (\varepsilon_1^e + \varepsilon_2^e + \varepsilon_3^e)^2 \qquad (3)$$
$$- 2(\varepsilon_1^e\varepsilon_2^e + \varepsilon_1^e\varepsilon_3^e + \varepsilon_2^e\varepsilon_3^e) = (\varepsilon_1^e)^2 + (\varepsilon_2^e)^2 + (\varepsilon_3^e)^2.$$

We now write an evolution equation for nonequilibrium parameter f in the form of the Landau–Khalatnikov equation

$$\tau_f \dot{f} = -\frac{\partial \Phi}{\partial f}, \qquad (4)$$

where τ_f is the relaxation time. In explicit form, it is written as

$$\tau_f \frac{\partial f}{\partial t} = -c\nabla^2 f + \varphi_0 - \varphi_1 f + \varphi_2 f^2 - \varphi_3 f^3. \qquad (5)$$

The lubricant temperature is determined in terms of the free energy of the system,

$$T \equiv -\frac{\partial \Phi}{\partial s} = 2\alpha s + \alpha_\varphi f. \qquad (6)$$

Thus, the entropy is a function of the temperature and excess volume, and free energy (1) is also a function of the temperature and volume.

To describe the heat exchange between the lubricant and the environment, we introduce friction surface temperature T_e [8]. In the case of nonuniform heating of the medium, the heat conduction equation represents an ordinary continuity equation [27],

$$T\frac{\partial s}{\partial t} = \kappa \nabla^2 T, \qquad (7)$$

where thermal conductivity κ is taken to be constant. The approximation

$$\kappa \nabla_z^2 T \approx \frac{\kappa}{h^2}(T_e - T),$$

where h is the lubricant thickness, can be used for normal component ∇_z^2 with an acceptable accuracy. As a result, Eq. (7) can be rewritten in the simpler form

$$\frac{\partial s}{\partial t} = \frac{\kappa}{h^2}\left(\frac{T_e}{T} - 1\right) + \frac{\kappa}{T}\nabla_{xy}^2 T, \qquad (8)$$

where h^2/κ plays the role of the relaxation time it takes for the temperatures across the lubricant thickness to be equalized due to heat conduction.

According to Eq. (1), elastic stresses are

$$\sigma_{ij}^e \equiv \frac{\partial \Phi}{\partial \varepsilon_{ij}^e} = \lambda\varepsilon_{ii}^e\delta_{ij} + 2\mu\varepsilon_{ij}^e - (\bar{\lambda}\varepsilon_{ii}^e\delta_{ij} + 2\bar{\mu}\varepsilon_{ij}^e)f. \qquad (9)$$

We can rewrite Eq. (9) in the form of effective Hooke's law

$$\sigma_{ij}^e = 2\mu_{\text{eff}}\varepsilon_{ij}^e + \lambda_{\text{eff}}\varepsilon_{ii}^e\delta_{ij} \qquad (10)$$

with effective elastic parameters

$$\mu_{\text{eff}} = \mu - \bar{\mu}f, \qquad (11)$$

$$\lambda_{\text{eff}} = \lambda - \bar{\lambda}f, \qquad (12)$$

which decrease upon melting as parameter f increases. The first and second invariants are determined by the standard procedure

$$\varepsilon_{ii}^e = \frac{n}{\lambda_{\text{eff}} + \mu_{\text{eff}}}, \qquad (13)$$

$$(\varepsilon_{ij}^e)^2 = \frac{1}{2}\left[\left(\frac{\tau}{\mu_{\text{eff}}}\right)^2 + (\varepsilon_{ii}^e)^2\right], \qquad (14)$$

where n and τ are the normal and tangential components of the stresses acting on the lubricant from the friction surfaces.[1] Equations (13) and (14) represent ordinary relationships between the tensor components and the tensor invariants of the linear theory of elasticity [26]. We use the Debye approximation, which relates elastic strain ε_{ij}^e to plastic strain ε_{ij}^{pl} [4],

$$\dot{\varepsilon}_{ij}^{pl} = \frac{\varepsilon_{ij}^e}{\tau_\varepsilon}, \qquad (15)$$

where τ_ε is the Maxwell time of internal-stress relaxation. The total strain in the layer is

---

[1] Shear stress τ is determined from Eq. (10) at $i \neq j$, i.e., $\delta_{ij} = 0$.

$$\varepsilon_{ij} = \varepsilon_{ij}^{e} + \varepsilon_{ij}^{pl}. \qquad (16)$$

This strain specifies the motion velocity of the upper block V_{ij} according to the relation [28]

$$V_{ij} = h\dot{\varepsilon}_{ij} \equiv h(\dot{\varepsilon}_{ij}^{e} + \dot{\varepsilon}_{ij}^{pl}). \qquad (17)$$

Using the last three relations, we write the following expression for the elastic component of the shear strain:

$$\tau_{\varepsilon}\dot{\varepsilon}_{ij}^{e} = -\varepsilon_{ij}^{e} + \frac{V_{ij}\tau_{\varepsilon}}{h}. \qquad (18)$$

The solution to this equation has the form

$$\varepsilon_{ij}^{e} = \left[\varepsilon_{ij}^{0} - \frac{V_{ij}\tau_{\varepsilon}}{h}\right]\exp\left\{-\frac{t}{\tau_{\varepsilon}}\right\} + \frac{V_{ij}\tau_{\varepsilon}}{h}, \qquad (19)$$

where ε_{ij}^{e} is the initial value of tensor ε_{ij}^{0}.

For simplicity, we will consider a homogeneous system and assume $\nabla \equiv 0$ in Eqs. (1), (5), and (8).

THERMODYNAMIC MELTING AND SHEAR MELTING

With regard to Eqs. (2), (6), (10)−(14), and (19), the system of kinetic equations (5) and (8) is a closed system and can be used to obtain graphical dependences of the quantities under study. In this section, we consider stationary states. According to Eqs. (8), (18), and (19), the lubricant temperature and the elastic component of the shear strain reach stationary values in the course of time,

$$T_0 = T_e, \quad \varepsilon_{ij0}^{e} = \frac{V_{ij}\tau_{\varepsilon}}{h}. \qquad (20)$$

To find the stationary states of all quantities, we have to numerically solve evolution equation (5) using Eqs. (2) and (10)−(14) and determine the current entropy from Eq. (6) at $T = T_e$ and the strain from Eq. (20).

In experiments, researchers often use atomically smooth mica surfaces as friction surfaces and spherical molecules of octamethyl cyclotetrasiloxane or linear chain molecules of tetradecane or hexadecane as a lubricant [2, 16]. These experiments were performed under the following conditions: the lubricant thickness was $h \approx 10^{-9}$ m; the contact area was $A \approx 3 \times 10^{-9}$ m²; and the load applied to the upper surface was $L = (2–60) \times 10^{-3}$ N, which corresponds to a normal stress $n = -L/A = -(6.67–200) \times 10^{5}$ Pa. The friction force was $F \approx (2–40) \times 10^{-3}$ N. As a result, researchers found that a lubricant melted when the temperature exceeded a certain critical value, $T_e > T_{c0} \approx 300$ K, or at a shear rate $V > V_c \approx 400$ nm/s. These critical values can change as a function of the type of lubricant and the experimental geometry.

According to the experimental data, we chose the following constants for our model:

$$\Phi_0^* = 20 \text{ J/m}^3, \quad \lambda = 2 \times 10^{11} \text{ Pa}, \quad \bar{\lambda} = 10^8 \text{ Pa},$$

$$\mu = 4.1 \times 10^{11} \text{ Pa}, \quad \bar{\mu} = 4 \times 10^{11} \text{ Pa}, \quad \varphi_0^* = 5 \text{ J/m}^3,$$

$$\varphi_1 = 1100 \text{ J/m}^3, \quad \varphi_2 = 2700 \text{ J/m}^3, \quad \varphi_3 = 2070 \text{ J/m}^3,$$

$$\alpha = 0.055 \text{ K}^2 \text{ m}^3/\text{J}, \quad \alpha_\varphi = 0.05 \text{ K}, \quad h = 10^{-9} \text{ m},$$

$$\tau_f = 1 \text{ Pa s}, \quad \tau_\varepsilon = 10^{-8} \text{ s}, \quad n = -7 \times 10^5 \text{ Pa}.$$

Note that the relaxation time of the excess volume τ_f has the dimension of viscosity. Actually, this means that the time it takes for a stationary friction mode to be reached increases with the effective viscosity.

Figure 1a shows the dependence of stationary excess volume f on friction surface temperature T_e at various shear rates V_{ij}. Let us analyze curve 1. It corresponds to a zero shear rate, and the shear stresses and strains are nil in this case. As the temperature increases, the excess volume increases monotonically; at $T_e = T_{c0}$, its value increases jumpwise and the lubricant melts. When the temperature decreases further, the lubricant solidifies at a lower temperature, $T_e = T_c^0$. This dependence has a hysteretic character, which corresponds to first-order phase transformations. As follows from Fig. 1a, the lubricant melts at a lower temperature as the shear rate increases. At a rate above a certain critical value, the lubricant is always liquid-like irrespective of the temperature (curve 4), which means the realization of one minimum in the $\Phi(f)$ dependence at high values of f.

Figure 2a shows the dependence of free energy Φ on excess volume f for the parameters of curve 1 in Fig. 1a. At low temperatures (upper curve), one minimum of the potential, which corresponds to a stationary state with a low value of f (solidlike lubricant), is operative. As the temperature increases (middle curve), a second minimum appears; however, the system cannot pass to the corresponding state because of the maximum between these minima. As T_e increases further, the separating maximum disappears, and the lubricant passes sharply (according to the mechanism of a first-order phase transformation) to the state corresponding to a single minimum at a high value of f; that is, the lubricant melts. If the temperature is now decreased, the system again cannot sharply pass into the corresponding state when the first minimum appears because of the separating maximum. When this maximum disappears at $T_e = T_c^0$, the lubricant solidifies jumpwise. The free energy in Fig. 2 is calculated as follows: the parameters (entropy, the first and second invariants, etc.) in a stationary state are first calculated; then, they are used for the calculation by Eq. (1), where only f is assumed to be an independent variable. After finding stationary states, Eq. (1) does not take into account term αs^2, since it does not affect the shape of the $\Phi(f)$ curve. However, as the temperature increases, this term strongly lowers this curve,

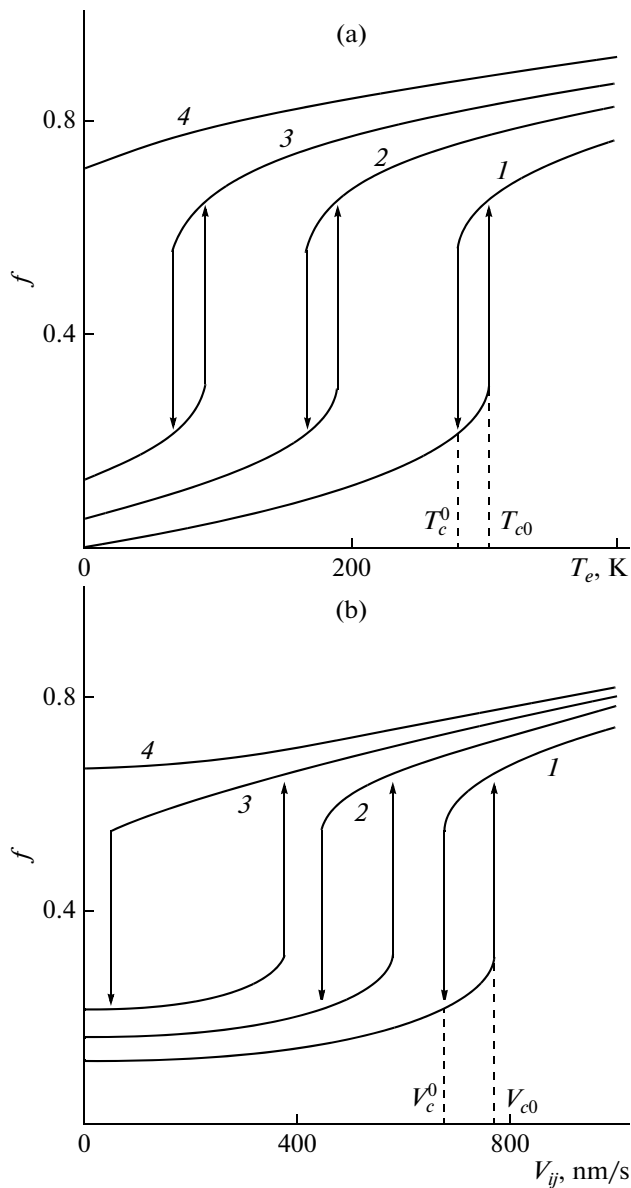**Fig. 1.** Dependences of stationary values of excess volume f on friction surface temperature T_e (K) and shear rate V_{ij} (nm/s). (a) Shear rate V_{ij} = (*1*) 0, (*2*) 800, (*3*) 1100, and (*4*) 1400 nm/s. (b) Friction surface temperature T_e = (*1*) 200, (*2*) 245, (*3*) 279, and (*4*) 310 K.

Fig. 2. Free energy density Φ (J/m^3) calculated by Eq. (1) vs. excess volume f. (a) Shear rate V_{ij} = 0 and temperature T_e = (*1*) 270, (*2*) 295, and (*3*) 310 K. (b) Temperature T_e = 200 K and shear rate V_{ij} = (*1*) 680, (*2*) 740, and (*3*) 800 nm/s.

which makes it impossible to place all three dependences in one figure.

Figure 1b shows stationary values of parameter f as a function of the shear rate at fixed T_e temperatures. It is seen that the lubricant melts when critical rate V_{c0} is exceeded and the lubricant solidifies at $V_{ij} < V_c^0$. The situation is similar to the behavior of the system when the temperature increases (Fig. 1a) with the difference that the area bounded by a hysteresis increases with the friction surface temperature in the case of shear melting. As a result, the energy losses for hysteresis, which
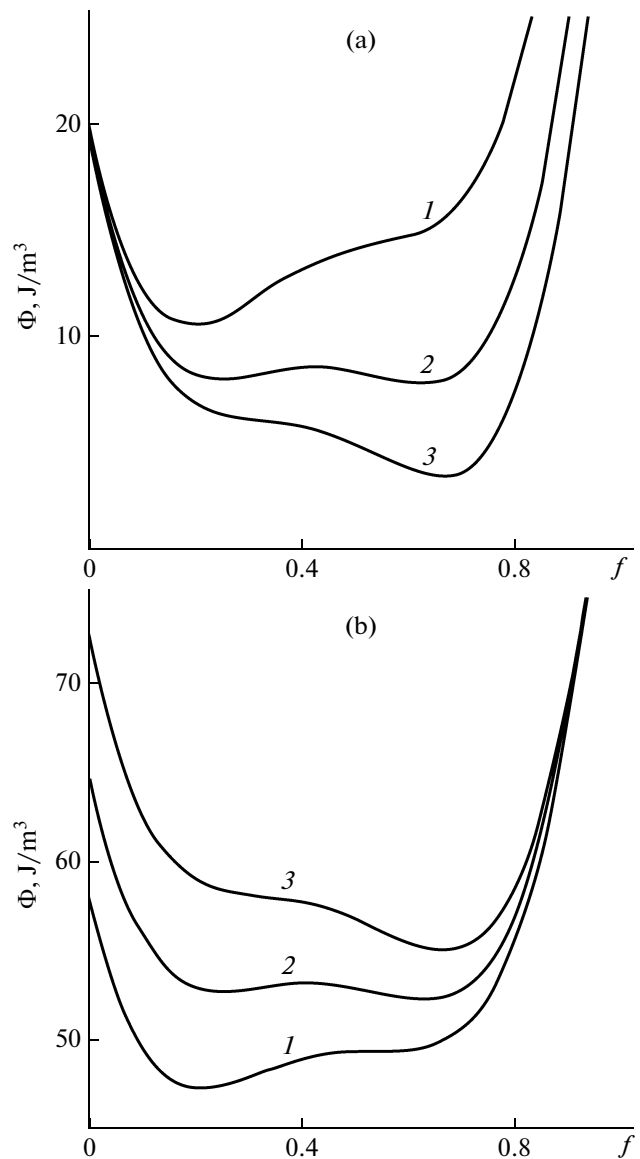
are proportional to the hysteresis area, grow. As the temperature increases, the lubricant melts at lower shear rates. Figure 2b shows the free energy profile at the parameters of curve *1* in Fig. 1b. This profile is seen to be similar to the energy profile during melting of the lubricant when the temperature increases. Thus, we can conclude that shear melting and thermodynamic melting are parts of the same process and that they should not be considered independently.

Figure 3a shows the dependences of critical melting rate V_{c0} and critical solidification rate V_c^0 of the lubricant on temperature T_e. Thus, above V_{c0}, the

lubricant is liquidlike and the sliding friction mode (*SF*) corresponding to a single $\Phi(f)$ minimum at high *f* takes place. Below the V_c^0 curve, the lubricant is solidlike, since there exists a single minimum of the free energy at such rates and low *f* (see Fig. 1b). Between the curves in Fig. 3a, there are two minima separated by a maximum in the $\Phi(f)$ curve (hysteresis region in Fig. 1, the middle curve in Fig. 2); that is, the state of lubricant is indefinite and depends on the initial conditions. Since any experimental system is heterogeneous, this region is most likely to contain a mixture of liquidlike and solidlike structures. However, to refine this circumstance, it is necessary to solve the partial differential equations given above at $\nabla \neq 0$, which is beyond the scope of this work.

According to Fig. 3a, both critical rates decrease until they become nil and full thermodynamic melting occurs as the temperature increases. Note that the lubricant melts even at zero temperature T_e if the shear rate exceeds the critical value (*SF* region boundary in the ordinate axis). As follows from the considerations given above, Fig. 3a represents a phase diagram with two stationary friction modes. The horizontal distance between the curves at $V_{ij} = $ const (segment *1*) is the hysteresis width that takes place in Fig. 1a at a constant rate, and the vertical distance at $T_e = $ const (segment *2*) is the hysteresis width at a constant temperature (Fig. 1b). As follows from Fig. 3a, the temperature hysteresis width (segment *1*) remains almost unchanged when the rate changes, and the rate hysteresis (segment *2*) becomes significantly broader as compared to low temperatures when the temperature increases. This fact is reflected in Fig. 1. Note that Fig. 3a can also be interpreted as the dependence of critical temperatures T_{c0} and T_c^0 on shear rate V_{ij}.

Figure 3b shows the temperature dependence of the hysteresis width depicted in Fig. 1b. This dependence was obtained when segment *2* in Fig. 3a was moved along the T_e axis. The hysteresis loop width increases over an almost entire temperature range. Its sharp decrease to zero is caused by the fact that, according to Fig. 3a, critical rate V_c^0 becomes zero at lower temperatures as compared to V_{c0}; after this moment, V_c^0 should be taken to be zero. Thus, the peak in Fig. 3b corresponds to the temperature at which rate V_c^0 vanishes. In the case of melting, the lubricant cannot solidify due to a decrease in the rate at such a temperature (according to Fig. 3a, the system at $V_c^0 = 0$ cannot be in region *DF*; however, it can initially be in the intermediate region and be solidlike at $V_{ij} < V_{c0}$). The temperature in Fig. 3b at which the hysteresis width becomes zero corresponds to the situation where the lubricant becomes liquidlike at any shear rate (as follows from Fig. 3a, the system in this
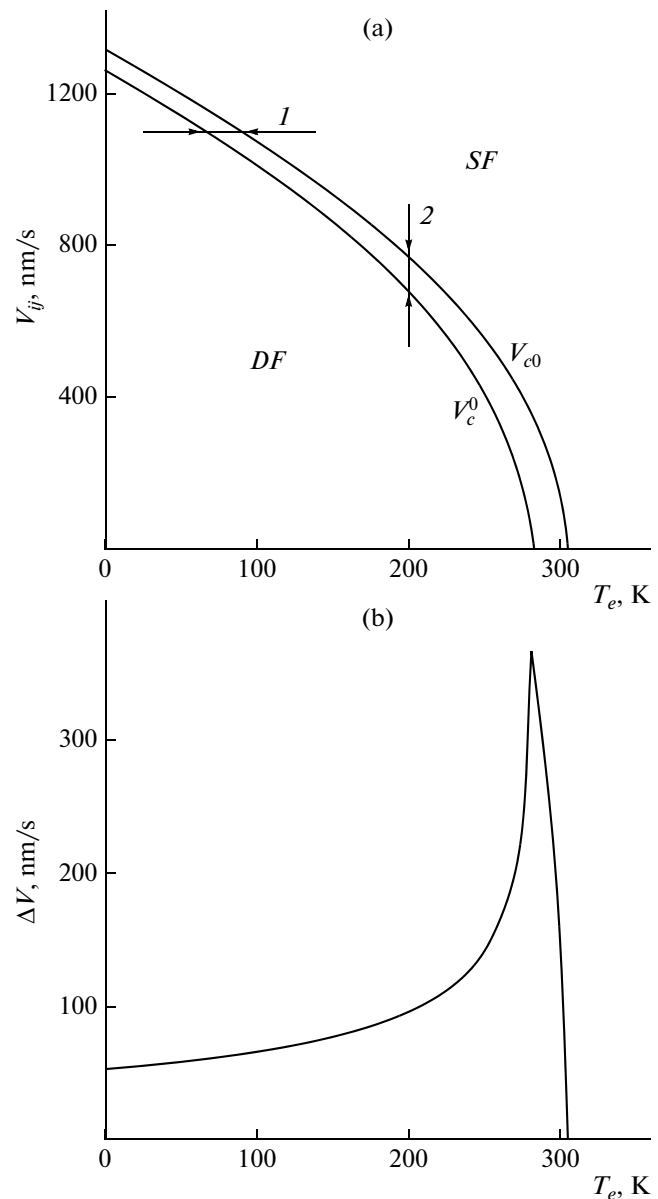

Fig. 3. (a) Phase diagram with sliding (*SF*) and dry (*DF*) friction regions. (b) Hysteresis width $\Delta V = V_{c0} - V_c^0$ (nm/s) vs. temperature T_e (K).

case is always in stick–slip friction region *SF*). The calculation of the dependence of the temperature hysteresis width $\Delta T_e = T_{c0} - T_c^0$ on rate V_{ij} demonstrates that it remains constant at all rates and $\Delta T_e \approx 25$ K except for the rates at which temperature T_c^0 is nil. As in the case shown in Fig. 3b, the hysteresis width vanishes monotonically as the rate increases (see Fig. 3a).

FRICTION FORCE

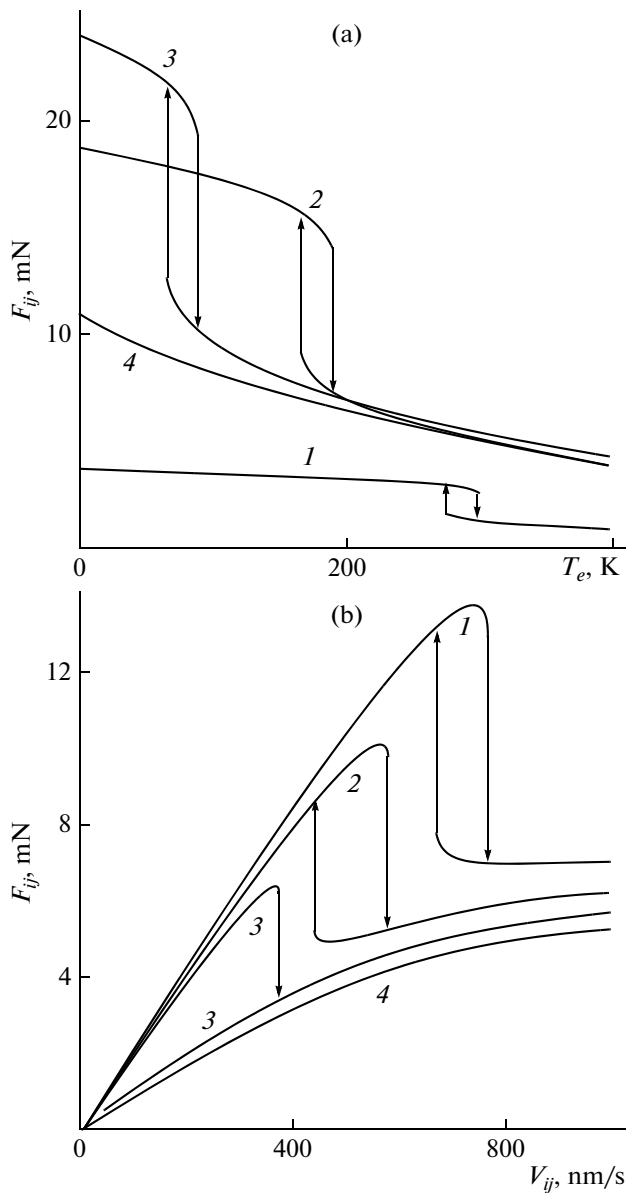In experimental works, researchers often present the dependences of the friction force on the shear rate,

Fig. 4. Dependences of friction force F_{ij} (mN) on shear rate V_{ij} (nm/s) and friction surface temperature T_e (K) at $\gamma = 2/3$ and a contact area $A = 3 \times 10^{-9}$ m^2. (a) Shear rate $V_{ij} = $ (*1*) 150, (*2*) 800, (*3*) 1100, and (*4*) 1400 nm/s. (b) Temperature $T_e = $ (*1*) 200, (*2*) 245, (*3*) 279, and (*4*) 310 K.

lubricant layer thickness, and normal pressure [1–3, 14–16]. In this section, we analyze the effect of the lubricant temperature and shear rate on the friction force.

Apart from elastic (σ_{ij}^e), viscous ($\sigma_{ij}^{\text{visc}}$) stresses appear in the lubricant. The total stress in the layer is the sum of these two contributions,

$$\sigma_{ij} = \sigma_{ij}^e + \sigma_{ij}^{\text{visc}}. \tag{21}$$

The total friction force is determined as usual,

$$F_{ij} = \sigma_{ij} A, \tag{22}$$

where A is the contact surface area. The viscous stresses in the layer are written as [28]

$$\sigma_{ij}^{\text{visc}} = \frac{\eta_{\text{eff}} V_{ij}}{h}, \tag{23}$$

where η_{eff} is the effective viscosity, which can only be found experimentally; for the boundary friction mode, we have

$$\eta_{\text{eff}} \propto (\dot{\varepsilon}_{ij})^{\gamma}, \tag{24}$$

where $\gamma = 2/3$ for most systems. Allowing for Eqs. (17) and (24), we rewrite Eq. (23) for the viscous stresses in the form

$$\sigma_{ij}^{\text{visc}} = \left(\frac{V_{ij}}{h}\right)^{\gamma+1}. \tag{25}$$

The final expression for the friction force is obtained upon the substitution of Eqs. (21) and (25) into Eq. (22),

$$F_{ij} = \left[\sigma_{ij}^e + \left(\frac{V_{ij}}{h}\right)^{\gamma+1}\right] A, \tag{26}$$

where σ_{ij}^e is specified by Eq. (10) at $i \neq j$.

Figure 4 depicts Eq. (26). All curves in Fig. 4a correspond to the parameters of the curves in Fig. 1a except for curve *1*, which is related to the fact that the first curve in Fig. 1a is plotted at a zero rate and that the friction force at rest is nil. All curves in Fig. 4b correspond to the curves in Fig. 1b.

Figure 4a illustrates the fact that the friction force decreases with increasing temperature. This behavior is caused by the fact that, as the temperature increases, parameter f increases; as a result, effective shear modulus $2\mu_{\text{eff}}$ (see Eq. (11)) decreases, which leads to a decrease in the elastic component of shear stresses (10) and, correspondingly, to a lower value of friction force (26). These dependences exhibit a hysteresis, since shear modulus (11) changes jumpwise upon a phase transition. At the parameters of curve *4*, the lubricant is always liquidlike and the friction force decreases with increasing temperature due to a decrease in the shear modulus (melting of the lubricant).

Figure 4b shows slightly different behavior. According to Eq. (26), the lubricant is solidlike at low shear rates and σ_{ij}^e is high (dry friction takes place). An increase in the rate in the dry friction mode leads to an increase in both components of friction force (26), and this force increases rapidly. As the shear rate increases further, the lubricant melts and elastic shear stresses (10) decrease substantially, which results in a further sharp decrease in the total friction force. If the rate still increases, F_{ij} increases due to the viscous component of the friction force, which increases with the shear rate. According to curve *4*, friction force (26) in the liquidlike state grows due to an increase in the shear rate. For clarity, we did not show the reverse hysteresis transition of the lubricant into the solidlike

state for curve *3* in Fig. 4b. This transition takes place at the break of curve *3* at low shear rates. Note that the results presented in Fig. 4b coincide qualitatively with the new friction map for the boundary friction mode obtained in [28] upon the generalization of experimental data.

CONCLUSIONS

We developed a theory that can describe the effects detected during the melting of an ultrathin lubricant film in the boundary friction mode. We considered both the ordinary case of thermodynamic melting induced by an increase in the temperature and shear melting due to the disordering caused by applied stresses. These two processes were shown to be interrelated, and they cannot be considered separately. For example, at a high friction surface temperature, shear melting begins at a lower shear rate (shear stresses); as the temperature increases further, the lubricant melts even at a zero shear rate (thermodynamic melting takes place).

We also considered the dependences of the friction force on the shear rate and temperature and, thus, took into account the effect of the temperature and shear melting. These are the main factors studied experimentally. Since our model is quantitative, its modifications can be used to describe certain experimental data.

ACKNOWLEDGMENTS

REFERENCES

1. B. N. J. Persson, *Sliding Friction: Physical Principles and Applications* (Springer, New York, 2000).
2. H. Yoshizawa and J. Israelachvili, J. Chem. Phys. **97**, 4128 (1993); J. Chem. Phys. **97**, 11300 (1993).
3. E. D. Smith, M. O. Robbins, and M. Cieplak, Phys. Rev. B **54**, 8252 (1996).
4. V. L. Popov, Zh. Tekh. Fiz. **71** (5), 100 (2001) [Tech. Phys. **46**, 605 (2001)].
5. J. M. Carlson and A. A. Batista, Phys. Rev. E **54**, 4153 (1996).
6. A. E. Filippov, J. Klafter, and M. Urbakh, Phys. Rev. Lett. **92** 135503 (2004).
7. Z. Tshiprut, A. E. Filippov, and M. Urbakh, Phys. Rev. Lett. **95**, 016101 (2005).
8. A. V. Khomenko and O. V. Yushchenko, Phys. Rev. E **68**, 036110 (2003).
9. O. M. Braun and A. G. Naumovets, Surf. Sci. Rep. **60**, 79 (2006).
10. R. G. Horn, D. T. Smith, and W. Haller, Chem. Phys. Lett. **162**, 404 (1989).
11. A. V. Khomenko and I. A. Lyashenko, Zh. Tekh. Fiz. **75** (11), 17 (2005) [Tech. Phys. **50**, 1408 (2005)].
12. A. V. Khomenko and I. A. Lyashenko, Zh. Tekh. Fiz. **77** (9), 137 (2007) [Tech. Phys. **52**, 1239 (2005)].
13. A. V. Khomenko and I. A. Lyashenko, Fluctuation Noise Lett. **7**, L111 (2007).
14. A. L. Demirel and S. Granick, J. Chem. Phys. **109**, 6889 (1998).
15. G. Reiter, A. L. Demirel, J. Peanasky, L. L. Cai, and S. Granick, J. Chem. Phys. **101**, 2606 (1994).
16. J. Israelachvili, Surf. Sci. Rep. **14**, 109 (1992).
17. A. V. Khomenko and I. A. Lyashenko, Fiz. Tverd. Tela (St. Petersburg) **49**, 886 (2007) [Phys. Solid State **49**, 936 (2007)].
18. A. V. Khomenko and I. A. Lyashenko, Phys. Lett. A **366**, 165 (2007).
19. L. S. Metlov, Deform. Razrush. Mater., No. 2, 40 (2007).
20. L. S. Metlov, Izv. Ross. Akad. Nauk, Ser. Fiz. **72**, 1353 (2008).
21. L. S. Metlov, Metallofiz. Noveishie Tekhnol. **29**, 335 (2007).
22. L. S. Metlov, Vestn. Donetsk. Univ., Ser. A: Estestv. Nauki, No. 1, 269 (2006).
23. A. V. Khomenko, I. A. Lyashenko, and L. S. Metlov, Metallofiz. Noveishie Tekhnol. **30**, 859 (2008).
24. P. A. Thompson, G. S. Grest, and M. O. Robbins, Phys. Rev. Lett. **68**, 3448 (1992).
25. M. L. Gee, P. M. McGuiggan, J. N. Israelachvili, and A. M. Homola, J. Chem. Phys. **93**, 1895 (1990).
26. L. M. Kachanov, *Foundations of the Theory of Plasticity* (Nauka, Moscow, 1969; North-Holland, Amsterdam, 1971).
27. L. D. Landau and E. M. Lifshitz, *Course of Theoretical Physics*, Vol. 7: *Theory of Elasticity* (Nauka, Moscow, 1987; URSS, Moscow, 2003).
28. G. Luengo, J. Israelachvili, and S. Granick, Wear **200**, 328 (1996).

Translated by K. Shakhlevich